



“Gheorghe Asachi” Technical University of Iasi, Romania



ECONOMICAL OPTIMIZATION OF AN INDIRECT SOLAR CABINET DRYER BASED ON MATHEMATICAL MODELING

Samaneh Sami¹, Amir Rahimi^{2*}, Nasrin Etesami¹

¹Isfahan University of Technology, Department of Chemical Engineering, Isfahan, Iran

²University of Isfahan, Faculty of Engineering, Department of Chemical Engineering, Isfahan, Iran

Abstract

This paper presents an optimization procedure to minimize the cost of drying in a solar cabinet dryer based on the results of a mathematical model. The model has been developed previously for performance analysis of a solar cabinet dryer. The optimal values for geometry of the solar collector, mass flux of air through the collector, and initial moisture content are obtained in a way that the drying cost is minimized. The results indicate that to optimize the drying cost, the best values of initial moisture content, air mass flux, the length and the surface area of collector are 9–10 kg/kg (dry basis), 0.03–0.045 kg/m².s, longer than 2.5 m, and 2.5–3 m², respectively. The results can help the designers to choose the optimum drying conditions for small scale industrial applications.

Key words: cost ratio, drying cost, optimum drying, solar energy

Received: December, 2011; *Revised final:* July, 2012; *Accepted:* July, 2012

1. Introduction

The use of solar thermal systems for the drying of various types of agricultural products has been proved to have many economic and environmental benefits. Solar dryers are classified into two categories: passive (natural convection) and active (forced convection). The natural drying process is based on temperature difference, and in consequence, the density difference of air inside the drying chamber. The density difference provides driving force (buoyant force) for the air that flows through the drying bed. The forced convection drying system requires mechanical or electrical power to provide air flow.

The construction of the passive drying system is simple, easy to maintain and inexpensive, where the working mechanisms are strongly dependent on temperature difference and pressure drop across the drying bed. Therefore, using the forced convection dryers such as indirect solar cabinet dryer saves time,

occupies less area, improves the product quality and hygiene, makes the process more efficient and protects the environment. Banout et al. (2011) compared a double-pass solar drier (DPSD) with a typical cabinet drier (CD) and a traditional open-air sun dryer for drying of the red chili.

Drying experiments are conducted for sponge-cotton; as a reference drying material in the ranges between 35.0 to 49.5 Å°C of ambient air temperature, 35.2 to 69.8 Å°C drying air temperature, 30 to 1258 W/m² solar radiation, and 0.016 to 0.08 kg/s drying air flow rate. For each experiment, the mass flow rate of the air remained constant throughout the day (Aissa, et al., 2014). The overall drying efficiencies of the DSPD and CD to reaching a desired moisture content of 10% (w.b) were 24.04% and 11.52%, respectively, while the overall drying efficiency of open-air sun drying to reach a desired moisture content of 15% (w.b) was 8.03%. Luminosu et al. (2012) tried to establish the optimum flow rate of the working fluid for the collector's area established by

* Author to whom all correspondence should be addressed: e-mail: rahimi@eng.ui.ac.ir; Phone +98 311 7934033; Fax +98 311 7934031

construction. In this way, the exergy efficiency is improved and the negative impact on the ambient environment is minimized. Ciocănea et al. (2011) presented the results of an experimental research on transient regimes of two types of solar air heat collectors. The absorbers of the collectors have different configurations and are made of different materials. Heat fluxes and efficiencies of collectors were computed for estimating the additional latent heat to be stored by the less efficient collector for increasing its performance to the level of the more efficient collector. Using results of such a study, the capacity of a given collector to store solar energy by using phase changing materials (PCM) can be assessed.

Due to these advantages, the solar drying is used extensively in industrial scale. Since the beginning of this millennium, using mathematical modeling technique to evaluate the performance of solar dryers has been developed. A verified mathematical model can be a valuable tool to saving cost and time.

Some researchers have conducted studies on the modeling of various drying processes (Forson et al., 2007; Ratti and Mujumdar, 1997). Janjai et al. (2008) presented experimental performance of solar drying of rosella flower and chili using roof-integrated solar dryer and also presented modeling of the roof-integrated solar dryer for drying of chili. Paraschiv et al. (2011) presented a computer modelling and experimental validation for the thermodynamic performance of parabolic trough solar collectors (PTSC) used in a micro-combined cooling heating and power (mCCHP) system. Hossain et al. (2005) optimized a solar tunnel drier for drying of chilli in Bangladesh. The simulation model was combined with the economic model of the solar tunnel drier and adaptive pattern search was used to find the optimum dimensions of the collector and the drying unit. An experimental study was conducted by Perasiriyana et al. (2013) to study the thin layer drying characteristics of vegetables and fish in a natural convection small scale solar tunnel dryer. The solar tunnel dryer was found to be more efficient than the open sundrying and resulted in saving to the extent of about 17.4% of drying time.

Several studies have been conducted on the optimization of solar drying systems, for both the forced convection and the natural convection situations (Bala and Woods, 1995; Mumba 1995; Simate, 2003; Samano Delgado et al., 2013). Simate (2003) combined solar drying simulation with the cost of the dryer materials and found the dryer dimensions for minimum drying cost.

The drying cost, annual cost and initial cost of the mixed-mode dryer were lower than those of the indirect-mode. Smitabhindu et al. (2008) tried to find the optimum values of structural and operational parameters of drying system so that the drying cost per unit of dried product is lowest. McDoom et al. (1999) optimized a scaled-down dryer by

recirculation the hot air and altering the degree of venting.

They could increase the energy saving up to 29 to 31%. Corzo et al. (2008) used response surface methodology to optimize the operating conditions of thin layer drying of coroba slices. Tasirin et al. (2007) presented the application of Taguchi method in optimizing the drying parameters of bird's eye chili in a fluidized bed dryer. Onyegegbu et al. (1994) simulated an integral type natural circulation solar crop dryer that would allow for the effects of varying ambient conditions of air temperature and humidity. Vega et al. (2009) considered the multi-objective dynamic optimization of fixed bed dryers. Very few studies have been conducted on providing the most suitable drying conditions on optimization of cost effective solar dryer. As an extension to our previous work (Sami et al., 2011a, 2011b), this study aims to optimize the performance of an indirect solar cabinet dryer based on mathematical modeling results.

Furthermore, the effects of main parameters such as solar collector length, solar collector surface area, mass flux of air, and initial moisture content of solid on the cost ratio are investigated. The optimum range of these parameters will be obtained for design purposes.

2. Mathematical model

Fig. 1 shows schematic diagram of an indirect cabinet solar dryer. The system consists of two parts: solar collector and drying chamber. The energy conservation law for the solar collector and the mass and energy conservation laws for the drying chamber are applied. The governing equations are presented in Table 1. It should be noted that in this equations the latent heat is not constant and it is a function of drying air temperature as appeared in Dissa et al. (2009).

Regarding the drying kinetic equation, $X_{eq,i}$ is a function of influent parameters such as temperature and relative humidity of gas.

It should be noted that in this case the internal mass transfer is controlling step. Furthermore, the temperature distribution within absorber plate has been neglected. More details about the model assumptions, the way to derive the equations, supplementary equations, and nomenclature are given in Sami et al. (2011b).

In our previous work (Sami et al., 2011b), the obtained ordinary differential equations and partial differential equations were solved numerically using the fourth order Runge-Kutta and the finite difference methods. The solution of the equations under unsteady state condition led to the profiles of humidity and temperature of drying air, and temperature and moisture content of drying solid versus time and length of dryer. The experimental data reported by Mohanraj et al. (2009) and Dissa et al. (2009) were used to validate the model. It should be noted that there is a difference between solar

collector applied by Mohanraj et al. (2009) and another one introduced by Dissa et al. (2009).

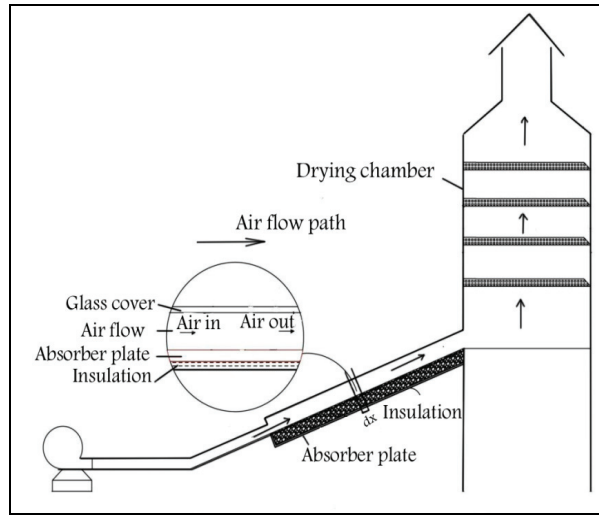


Fig. 1. Schematic of the indirect solar cabinet dryer

The collector in (Mohanraj et al., 2009) study includes a storage material under the absorber plate. The results (Sami et al., 2011b) revealed the necessity to optimize the dryer component and drying process, which is addressed in this study in detail.

3. Optimization model

The cost of a solar dryer consists of the costs of solar collector and drying chamber. Here, the objective function is defined as the ratio of the cost of a solar supplemented system to the cost of an electrical drying system, namely (Eq. 1). The defined cost ratio is always less than unity.

$$CR = \frac{C_s}{C_e} \quad (1)$$

In fact, low cost of a solar supplemented system is an advantage for further application of the solar systems. The amount of useful energy required per unit of product per day can be estimated as the useful amount of energy required for sensible heating of product and useful amount of energy required for evaporation of moisture in the product (Purohit, et al., 2006), namely (Eq. 2):

$$E_f = \frac{1 + X_i}{1 + X_f} \{1 + (\tau - 1)\xi\} \sum_{i=1}^N C_p (T_{o,i} - T_{in,i}) + \left\{ \frac{X_i - X_f}{1 + X_f} \right\} h_{fg} \quad (2)$$

The annual energy consumption is achieved by adding the amounts of energy needed for a day over a year. The corresponding annual cost of electrical energy is defined as follows (Eq. 3):

$$C_e = E_f S_e \quad (3)$$

The cost of an electrical drying system can be calculated by summing the annual cost of electrical energy (Eq. (3)) and the total cost of a solar supplemented system (C_s).

The total cost of solar supplemented system are represented as the annual cost per unit weight of solid dried per year (Eq. 4) (Radajewski, et al., 1987):

$$C_s = \frac{C_a}{m_d} \quad (4)$$

3.1. Annual cost calculation

It is necessary to specify the annual cost (C_a) in the total cost of solar supplemented system (C_s) equation.

Table 1. Governing equations of solar dryer

	Name of equation	Equation
Equations of solar collector	Energy balance on glass cover	$\frac{\partial T_g}{\partial t} = \left(\frac{k_g}{\rho_g C_g} \right) \frac{\partial^2 T_g}{\partial z^2} + \frac{I_t \alpha_g}{\rho_g C_g \delta}$
	Energy balance on absorber plate	$\frac{\partial T_p}{\partial t} = \frac{I_t \tau_g \alpha_p}{\rho_p C_p l_p} + \left(\frac{h_{pa}}{\rho_p C_p l_p} \right) (T_a - T_p) - \frac{h_{rpsky}}{\rho_p C_p l_p} (T_p - T_{sky}) - \frac{h_{rpg}}{\rho_p C_p l_p} (T_p - T_g)$
	Energy balance on the air stream	$\frac{\partial T_a}{\partial t} = -u \frac{\partial T_a}{\partial x} + \frac{h_{ga} b}{\rho_a C_a A_c} (T_g - T_a) + \frac{h_{pa} b}{\rho_a C_a A_c} (T_p - T_a)$
Equations of drying chamber	Energy balance on the air flow on each tray	$\frac{\partial T_i}{\partial t} = -\frac{\dot{m}_a C_{pm}}{S \varepsilon L \rho_a C_a} (T_i - T_{i-1}) - \frac{h_a a}{\varepsilon \rho_a C_a} (T_i - T_{s,i})$
	Mass balance on the air flow on each tray	$\frac{\partial H_i}{\partial t} = -\frac{\dot{m}_a}{S \varepsilon L \rho_a} (H_i - H_{i-1}) - \frac{m_s}{S \varepsilon L \rho_a} \left(\frac{\partial X_i}{\partial t} \right)$
	Energy balance on the solid slices on each tray	$\frac{\partial T_{s,i}}{\partial t} = \frac{m_s \lambda}{SL(1-\varepsilon)\rho_s C_s} \left(\frac{\partial X_i}{\partial t} \right) + \frac{h_a a}{(1-\varepsilon)\rho_s C_s} (T_i - T_{s,i})$
	Relation for drying kinetics (Dissa et al, 2009)	$\frac{\partial X_i}{\partial t} = -0.000026(X_0 - X_{eq,i}) \exp(-2.567 \times 10^{-5} t)$
	Relation for drying kinetics (Mohanraj et al, 2009)	$\frac{\partial X_i}{\partial t} = -K(X_i - X_{eq,i})$

The annual cost is defined as the following equation (Eq. 5): (Audsley and Wheeler, 1978):

$$C_a = \left(C_T + \sum_{i=1}^N C_{m,i} \omega^i \right) \frac{(\omega - 1)}{\omega(\omega^N - 1)} \quad (5)$$

where: ω is expressed as follow (Eq. 6):

$$\omega = \frac{100 + i_{\text{interest}}}{100 + i_{\text{inflation}}} \quad (6)$$

According to the above equation, the annual cost depends on the maintenance cost, total fixed cost of drying per year, interest and inflation rates. The maintenance cost C_m is assumed to be 2% of the total fixed cost of drying per year (Simate, 2003).

3.2. The total fixed cost of drying calculation

In order to calculate the annual cost by Eq. (5), it is necessary to define the total fixed cost of drying per year. The mentioned parameter can be expressed as follows (Eq. 7):

$$C_T = C_r + C_F + C_l + C_i \quad (7)$$

Therefore, the total fixed cost of drying consists of depreciation cost (C_r), cost of fan (C_F), cost of labor (C_l) and interest (C_i). Each of these values will be explained in detail.

3.2.1. Depreciation cost

The main components of a solar dryer are collector, drying chamber and a fan for air flow in the system. Each of these parts has its own annual depreciation cost that determines the total depreciation cost (Eq. 8):

$$C_r = \frac{C_d}{L_d} + \frac{C_c}{L_c} + \frac{C_b}{L_b} \quad (8)$$

where: L_d , L_c and L_b are effective life time of drying chamber, solar collector and fan, which are characterized by 5, 5 and 2 years, respectively; C_d is the fixed cost of drying chamber.

The depreciation cost of the fan (C_b) can be calculated by Eq. (9) (Radajewski et al., 1987):

$$C_b = 155 (\nu_c + 1.43) \quad (9)$$

The cost of the solar collector (C_c) in Eq. (8) is calculated by Eq. (10):

$$C_c = S_c A_c + S_p z_1 + S_d z_2 \quad (10)$$

where, z_1 and z_2 are plenum and air-duct size factors (m^2), respectively calculated from collector geometry and the rate of air flow through the collector as follows (Eq. 11 and 12) (Radajewski et al., 1987):

$$z_1 = 1.2w(\sin \theta + \cos \theta) + \frac{\omega^2}{2} \sin 2\theta \quad (11)$$

$$z_2 = 4w \cos \theta \left(\frac{G_a A_c}{7\rho_a} \right)^{1/2} \quad (12)$$

3.2.2. Cost of fan

Cost of the fan is a function of fan nominal power and is calculated by (Eq. 13):

$$C_F = P_f t S_e \quad (13)$$

The nominal fan power is also a function of total pressure drop and volumetric flow rate of flowing air. Eq. 14 is used to estimate the nominal fan power:

$$P_f = \frac{QP_t}{1000 \eta_f} \quad (14)$$

The nominal power shows the electricity consumption of fans or pumps. The fan efficiency is assumed to be 65%. The volumetric flow rate through the collector is defined as follows (Eq. 15):

$$Q = \frac{G_a l_c w}{\rho_a} \quad (15)$$

3.2.2.1. Total air pressure drop

Here, the method proposed by Kreith and Kreider (1978) is used to calculate the total air pressure drop. They introduced Eq. (16):

$$P_t = P_1 + P_2 + P_3 + P_4 + P_5 \quad (16)$$

where: P_1 is the pressure drop due to the contraction of air flow at the collector inlet (Eq. 17):

$$P_1 = 0.55(\rho_a \nu_c^2 / 2) \quad (17)$$

The air velocity within collector is given by Eq. (18):

$$\nu_c = G_a l_c / s \rho_a \quad (18)$$

The pressure drop within the air space of the collector (P_2) is given by Darcy equation (19):

$$P_2 = \rho_a f l_c \nu_c^2 / 2d_h \quad (19)$$

where, the friction factor is determined by Eqs. (20) and (21) (Moody and Princeton, 1944):

$$f = \left(-2 \log \left(\Phi / 3.7 + 2.51 / f^{1/2} \text{Re} \right) \right)^{-2} \quad \text{Re} > 3000 \quad (20)$$

$$f = 64 / \text{Re} \quad \text{Re} < 3000 \quad (21)$$

P_3 is the air pressure drop at the collector outlet and can be estimated by Eq. (22):

$$P_3 = (1 - w_s / (w^2 \sin(2\theta) / 4))^2 \rho_a v_c^2 / 2 \quad (22)$$

The pressure drop at the chamber inlet (P_4) can be calculated by Eq. (23):

$$P_4 = 0.55(1 - v_a / w \gamma \cos \theta)^2 \rho_a v_c^2 / 2 \quad (23)$$

γ is the product of air velocity through the plenum duct, which is constant (equal to 8.4 m²/s). Finally, the air pressure drop in the drying chamber, P_5 is defined by (Eq. 24):

$$P_5 = 2l_d \tau \rho_a v_a^2 / d_d \quad (24)$$

Knowing the solar dryer operating and geometrical characteristics, the values of P_1 to P_5 are calculated. The total air pressure drop in the system is then calculated by (Eq. 16).

3.2.3. Cost of labor

Another factor in calculating the total fixed cost of the drying per year is cost of labor which is calculated by Eq. (25):

$$C_l = t_d D_a S_l \quad (25)$$

3.2.4. Interest

Interest on the capital investment is calculated by multiplying a real interest rate in the average written down value of the equipment (Eq. 26):

$$C_i = i(C_d + C_b + C_c) / 2 \quad (26)$$

4. Optimization procedure

The cost of the main construction materials including timber, glass and wire mesh in January 2011 in Iran were 11.90, 9.20, and 6.13 US \$/m², respectively. The interest and inflation rates were 15% and 12%, respectively. In a direct unit, the cost of glass and timber are the main material costs, whereas for an indirect-mode dryer unit, the main material is timber. In addition, for both kinds of drying units the cost of the wire mesh is common.

Using the previous model (Sami et al., 2011b), the effect of operating and geometrical parameters on the performance of a cabinet solar dryer is investigated. The cost ratio as the objective function is calculated. Minimizing the cost ratio is the main aim of this study.

5. Results and discussion

In this section, the effect of several parameters on the cost ratio in a solar dryer is determined. The solar dryer applied is similar to that used in Dissa's study (2009). Fig. 2 shows the effect of air mass flux on the cost ratio for three various initial moisture contents. In Fig. 2, S is distance between glass cover

and absorber plate and I_c is length of collector. By increasing the air mass flux, the total pressure drop increases, and therefore, the depreciation cost of the fan increases. This yields to increase the total fixed cost of the drying system. In Fig.2, the cost ratio is decreased. If the air mass flux is increased too much, energy supplied for drying (E_f) decreases because the difference between the inlet and outlet air temperature suddenly decreases. According to Eq. (3), the cost of the electrical system (C_e) is directly proportional to the energy supplied for drying (E_f), which leads to an increase in the cost ratio.

So, initially the cost ratio decreases and then increases. It can be concluded that the optimum value of cost ratio is achieved when the air mass flux is between 0.035 and 0.045 kg/m².s. According to Fig. 2, the cost ratio decreases with an increase in the initial moisture content. The supplied energy (E_f) defined in Eq. (2), increases by increasing the initial moisture content. Therefore, the amount of cost ratio decreases. Optimum amount of air mass flux for initial moisture content of 5, 6.5 and 8.5 (d.b) is obtained as 0.039, 0.0362 and 0.035 kg/m².s, respectively. The variation of the cost ratio as a function of initial moisture content for three values of air mass fluxes is illustrated in Fig. 3. In lower initial moisture contents, the cost ratio is decreased along with the initial moisture content because of increasing the supplied energy (Eq. 2) and cost of electrical system.

In higher initial moistures, the amount of total fixed cost as well as the cost of fan operation increases due to increasing the drying time duration ($t_d \delta$). According to Fig. 3, the optimum amount of initial moisture content for air mass flux of 0.015, 0.035, and 0.055 kg/m².s is 9.7, 9.8, and 10 (d.b), respectively. The optimum value of cost ratio is when the initial moisture content varies between 9 and 10.5 (d.b).

The variation of the cost ratio with the length of the solar collector for three values of air mass fluxes is shown in Fig. 4. The outlet air temperature increases when the length of the collector is increased. Therefore, for the same outlet air temperature, the cost of electrical system (C_e) increases, and the cost ratio decreases. The slope of profiles of the cost ratio for longer collectors is lower. In fact, further increase in the collector length increases the air total pressure drop, the fan operating cost, and the total fixed cost. Hence, the cost of solar supplemented system highly increases. The optimum lengths for collector corresponding to the refereed air mass fluxes in Fig. 4 are 3.12, 3 and 2.712 m, respectively. Designers may achieve the optimum value of the cost ratio when the collector length is more than 2.5 m.

Fig. 5 shows the effect of air mass flux on the cost ratio for three values of collector length. The variation of the cost ratio with air mass flux is similar to Fig. 2. The optimum amount of air mass flux for collector length of 3.5, 3 and 2.5 m is 0.04, 0.03 and 0.0345 kg/m².s, respectively. Designers can realize

that the optimum value of the cost ratio is achieved in 0.03–0.045 kg/m².s. This optimum range is very close to that obtained in Fig. 2.

Fig. 6 shows the effect of initial moisture content on the optimum cost ratio for different values of collector length, including 2.5, 3 and 3.5 m. There is a certain optimal value for fixed throughput systems. The dependency of cost ratio on initial

moisture content is qualitatively similar to the other characteristic factors. Fig. 6 reveals a clear minimum value for cost ratio while the initial moisture content is between 8 and 9.5. When the initial moisture content is less than 8, the cost savings will be less since there is low use of the capital invested in the solar equipment.

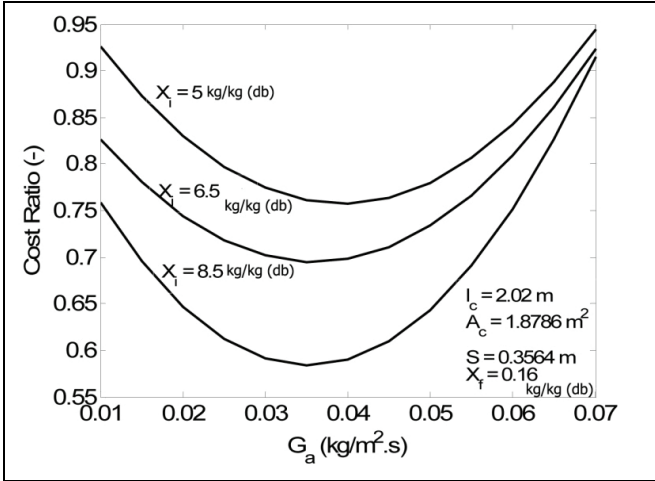


Fig. 2. Variation of the cost ratio with the air mass flux

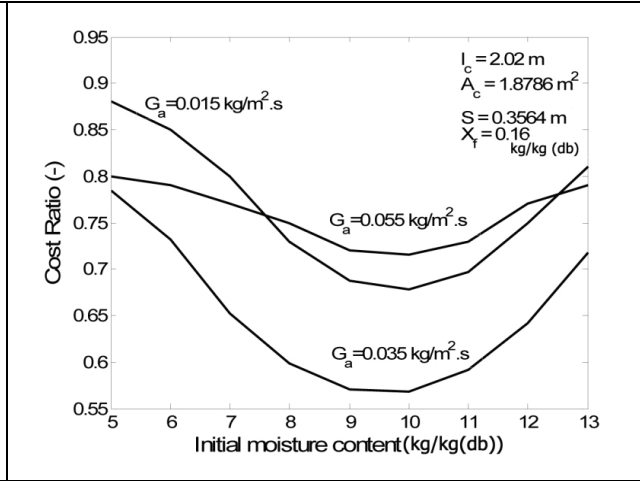


Fig. 3. Variation of cost ratio with the initial moisture contents in three different air mass flux

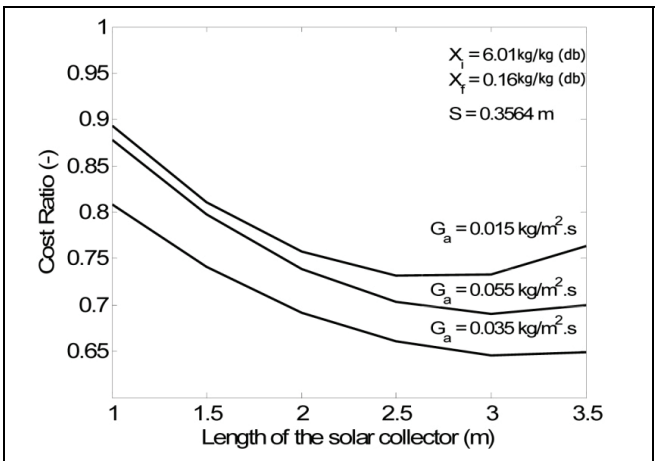


Fig. 4. Variation of cost ratio with the solar collector length in three air mass fluxes

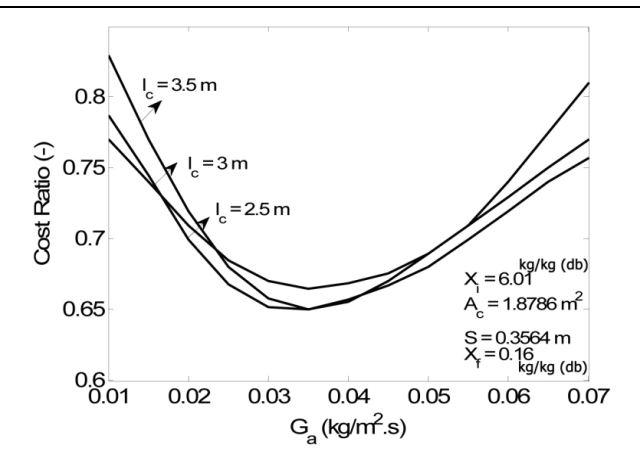


Fig. 5. Variation of cost ratio with the air mass flux in three different lengths of solar collector

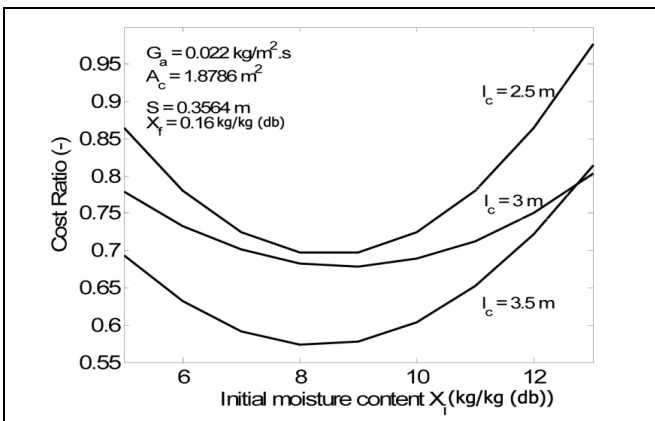


Fig. 6. Variation of cost ratio with the initial moisture contents in three lengths of solar collector

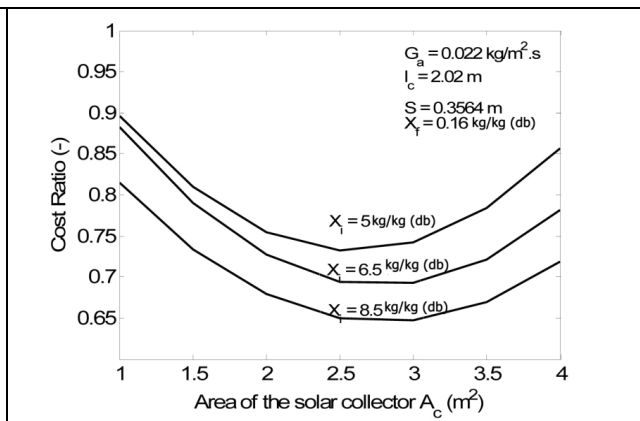


Fig. 7. Variation of cost ratio with area of solar collector in three initial moisture contents

In fact, for drying materials with low initial moisture content, the total heat requirement is small and the operation time is short. Therefore, the contribution of solar systems is small. At higher initial moisture contents (> 9.5), the drying time is longer. Hence, the contribution of solar systems is again small.

The optimum values of initial moisture content for collector lengths of 2.5, 3 and 3.5 m are obtained to be 8.65, 8.95 and 8.32 (d.b), respectively. Fig. 7 shows the variation of cost ratio with the solar collector surface area for three values of initial moisture contents. When the collector surface area is small ($< 2.5 \text{ m}^2$), increasing the surface area of the collector rises the outlet air temperature. Hence, the cost of electrical system increases and the cost ratio decreases. For collectors with larger surface area ($> 3 \text{ m}^2$), an increase in the surface area leads to increase the total pressure drop. Hence, a sudden increase in the total fixed cost of drying is observed, and the cost ratio increases. The optimal values of solar collector area for initial moisture contents of 5, 6.5 and 8.5 are 2.6, 2.75 and 3 m^2 , respectively. The optimal value of cost ratio is achieved in the range of $2.5\text{--}3 \text{ m}^2$ of collector surface area. Fig. 8 illustrates the variation of cost ratio with dryer throughput per a drying batch obtained in two different experimental systems.

These experimental systems are the same as those applied by Mohanraj et al. (2009) and Dissa et al. (2009) and there is only a structural difference between them. In the system used by Mohanraj and coworkers an energy storage material is used under the absorber plate. In the previous study (Sami et al., 2011b), the experimental data obtained by these researchers have been used in order to validate the new presented mathematical model.

A comparison is made in Fig. 8 for a same dryer throughput. This Figure shows that for dryer throughput less than 8 kg/batch, the cost savings are reduced, since the drying time is shorter and there is low use of the capital invested in the solar equipment.

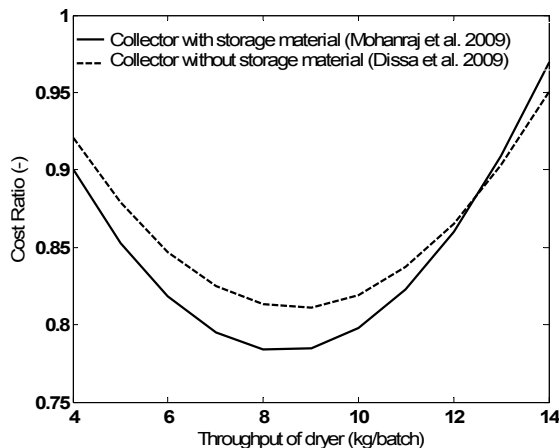


Fig. 8. Effect of the usage of storage material in collector structure on the cost ratio

For dryer throughput greater than 9.5 kg/batch the cost ratio is enhanced. In this situation, total time of a day that the drying operation is performed increases and therefore, the contribution of solar energy is decreased. Furthermore, Fig. 8 indicates that the maximum solar energy is utilized in Mohanraj's system due to the existing of the storage material. This means that in the Dissa's dryer the drying process is longer.

Therefore, the cost of electrical system and depreciation cost in Dissa's dryer is more than that of the Mohanraj's dryer. This result indicates that the thermal efficiency and economical benefits of Mohanraj' dryer is more than that used by Dissa et al. (2009), and as expected, the amount of cost ratio is found to be less than that of the Dissa's dryer.

6. Conclusions

In this work, the optimization and analysis of an indirect solar cabinet dryer was conducted based on the results of a mathematical model. An objective function was defined as the cost of a solar supplemented system to the cost of an electrical dryer system.

The effect of various parameters on cost ratio is considered in detail. In addition, the optimum range for each one of the parameters was estimated based on the obtained results.

The optimum ranges of initial moisture content; air mass flux, collector length and surface area were obtained as 9–10 d.b, $0.03\text{--}0.045 \text{ kg/m}^2\cdot\text{s}$, longer than 2.5 m, and $2.5\text{--}3 \text{ m}^2$, respectively. Furthermore, the obtained results indicate that using an energy storage material under the absorber plate of the collector can reduce the cost ratio of the dryer significantly.

Acknowledgements

We owe a debt of gratitude to professor Mohanraj and professor Dissa for their permission to use their experimental results in this paper. We extend our thanks to Mr. Mohanraj for sending us the details of his solar dryer properties.

Nomenclature

A_c	collector surface area (m^2)
CR	cost ratio or objective function (–)
C_a	annual cost (\$/year)
C_b	depreciation cost of fan (\$)
C_c, C_d	depreciation cost of solar collector and drying chamber, respectively (\$)
C_e, C_f, C_m	cost of electrical system, fuel, fan, and maintenance, respectively (\$/kg)
C_p	specific heat of air ($\text{kJ/kg}\cdot\text{C}$)
C_s	total cost of drying, solar supplemented system (\$/kg)
C_T	total cost of drying (\$/year)
D_a	length of drying period (d/a)
d_d	drying chamber width (m)
d_h	hydraulic diameter (m)
E_f	total energy required for drying (kJ/kg)

f	friction factor (–)
G_a	air mass flux (kg/m ² .s)
h_{fg}	latent heat of vaporization (kJ/kg)
i	interest rate (–)
$i_{inflation}$	inflation rate (–)
L_d, L_c, L_b	life time of drying chamber, collector, and fan, respectively (year)
l_c, l_d	length of collector and drying chamber, respectively (m)
\dot{m}_a	mass flow rate of air (kg/s)
m_d	drying capacity per year (kg)
N	number of interval time per day (–)
P_f	power of fan (kW)
P_t	total pressure drop (kg/m.s ²)
Q	flow rate through collector (m ³ /s)
S	distance between glass cover and absorber plate (m)
S_c, S_d, S_p	specific cost of collector, drying chamber, and plenum, respectively (\$/m ²)
S_e	specific cost of electricity (\$/kJ)
S_l	specific cost of labor (\$/h)
T_i, T_o	inlet and outlet collector air temperature, respectively (K)
t_d	number of hours of drying per day (h)
t	Time of drying per kg of production (s/kg)
v_a, v_c	velocity through drying chamber and collector, respectively (m/s)
w	width of collector (m)
X_i, X_f	initial and final moisture content, respectively (d.b)
z_1, z_2	plenum and air–duct size factors (m ²)
ξ	fraction of the sensible heating requirement of the product on the first day that is required for sensible heating on other days of drying
τ	time required for drying of a single batch of the product (day)
ρ_a	density of air (kg/m ³)
Φ	relative roughness (–)
θ	slope of the collector (rad)

References

- Aissa W., Ei-Sallak M., Elhakem A., (2014), Performance of solar dryer chamber used by convective drying of Spong-Cotton, *Thermal Science*, **18**, S451-S462.
- Audsley E., Wheeler J., (1978), The annual cost of machinery calculated using actual cash flows, *Journal of Agricultural Engineering Research*, **23**, 189-201.
- Bala B. K., Woods J. L., (1995), Optimization of natural-convection, solar drying systems, *Energy*, **20**, 285-294.
- Banout J., Ehl P., Havlik J., Lojka B., Polesny Z., Verner V., (2011), Design and performance evaluation of a Double-pass solar drier for drying of red chilli (*Capsicum annum* L.), *Solar Energy*, **85**, 506-515.
- Ciocănea A., Dragomirescu A., Budea S., (2011), Experimental research on transient regimes of solar air heat collectors, *Environmental Engineering and Management Journal*, **10**, 1097-1103.
- Corzo O., Bracho N., Vsquez A., Pereira A., (2008), Optimization of a thin layer drying process for coroba slices, *Journal of Food Engineering*, **85**, 372-380.
- Dissa A.O., Bathiebo J., Kam S., Savadogo P.W., Desmorieux H., Kouliadiati J., (2009), Modelling and experimental validation of thin layer indirect solar drying of mango slices, *Renewable Energy*, **34**, 1000-1008.
- Forson F.K., Nazha M.A.A., Rajakaruna H., (2007), Modelling and experimental studies on a mixed-mode natural convection solar crop-dryer, *Solar Energy*, **81**, 346-357.
- Kreith F., Kreider J. F., (1978), Principles of Solar Energy, McGraw-Hill Book Company, New York.
- Kulkarni G.N., Kedare S.B., Bandyopadhyay S., (2007), Determination of design space and optimization of solar water heating systems, *Solar Energy*, **81**, 958-968.
- Luminosu I., Fara L., Pop N., Costachel M., Fara S., (2012), Exergy Analysis of the air solar collector based on experimental data, *Environmental Engineering and Management Journal*, **11**, 1367-1374.
- McDoom I.A., Ramsaroop R., Saunders R., Kai A.T., (1999), Optimization of solar crop drying, *Renewable Energy*, **16**, 749-752.
- Michelson E., (1982), Multivariate optimization of a solar water heating system using the Simplex method, *Solar Energy*, **29**, 89-99.
- Mohanraj M., Chandrasekar P., (2009), Performance of a forced convection solar dryer integrated with gravel as heat storage material for chili drying, *Journal of Engineering Science and Technology*, **4**, 305-314.
- Moody L.F., Princeton N.J., (1944), Friction factors for pipe flow, *Transactions of American Society of Mechanical Engineers*, **66**, 671-684.
- Mumba J., (1995), Economic analysis of a photovoltaic, forced-convection, solar grain drier, *Energy*, **20**, 923-928.
- Onyegegbu S.O., Morhenne J., Norton B., (1994), Second law optimization of integral type natural circulation solar energy crop dryers, *Energy Conversion and Management*, **35**, 973-983.
- Paraschiv S., Ion I.V., Paraschiv L.S., (2011), Thermodynamic performance for the solar collector of a Micro-Combined cooling, heating and power system, *Environmental Engineering and Management Journal*, **10**, 1311-1317.
- Perasiriyan V., Karthikadevi B., Sivakumar T., (2013), Optimization of drying process for vegetables and fish by solar tunnel dryer, *International Journal of Food, Agriculture and Veterinary Sciences*, **3**, 51-57.
- Purohit P., Kumar A., Kandpal T. C., (2006), Solar drying vs. open sun drying: A framework for financial evaluation, *Solar Energy*, **80**, 1568-1579.
- Radajewski W., Jolly P., Abawi G. Y., (1987), Optimization of solar grain drying in a continuous flow dryer, *Journal of Agricultural Engineering Research*, **38**, 127-144.
- Ratti C., Mujumdar A.S., (1997), Solar drying of foods: Modeling and numerical simulation, *Solar Energy*, **60**, 151-157.
- Samano Delgado E., Martinez-Flores H.E., Garnica-Romo M.G., Aranda-Sanchez J.I., Sosa-Aguirre C.R., Cortes-Penagos C.D.J., Fernandez-Munoz J.L., (2013), Optimization of solar dryer for the dehydration of fruits and vegetables, *Journal of Food Processing and Preservation*, **37**, 489-495.
- Sami S., Etesami N., Rahimi A., (2011a), Energy and exergy analysis of an indirect solar cabinet dryer based on mathematical modeling results, *Energy*, **36**, 2847-2855.
- Sami S., Rahimi A., Etesami N., (2011b), dynamic modeling and a parametric study of an indirect solar

- cabinet dryer, *Drying Technology: An International Journal*, **29**, 825-835.
- Simate I.N., (2003), Optimization of mixed-mode and indirect-mode natural convection solar dryers, *Renewable Energy*, **28**, 435-453.
- Smitabhindu R., Janjai S., Chankong V., (2008), Optimization of a solar-assisted drying system for drying bananas, *Renewable Energy*, **33**, 1523-1531.
- Tasirin S.M., Kamarudin S.K., Ghani J.A., Lee K.F., (2007), Optimization of drying parameters of bird's eye chilli in a fluidized bed dryer, *Journal of Food Engineering*, **80**, 695-700.
- Vega M.P., Mancini M.C., Calçada L.A., Jacek J., Jan T., (2009), *Multi-Objective Dynamic Optimization of Fixed Bed Dryers: Simulation and Experiments*, Elsevier, Amsterdam.